Characterization of Particulate Matter Containing Various Organic Components

HONORS RESEARCH THESIS

Presented in Partial Fulfillment of the Requirements of the *graduation with research distinction* in Chemistry in the undergraduate colleges of The Ohio State University

By

Christophe Isaac Robitaille

Undergraduate Honors Thesis Program in Chemistry

The Ohio State University

2011

Honors Thesis Committee: Assistant Professor Anne Co and Professor Joseph Williams

Project Advisor: Professor James V. Coe, Department of Chemistry

Abstract

Particulate matter is ubiquitous in the atmosphere and is known to have significant effects on the pulmonary and cardiovascular systems, as well as less acute generalized systemic responses. While many studies have focused on the concentration of particulate matter, it is also essential to consider the composition of such species. Characterization of dust presents some challenges as the particles of interest have sizes on the order of the wavelengths of light, leading to substantial scattering, which complicates absorption spectra. Scatter-free infrared spectra may be obtained from single particles on the order of 5 μm by utilizing the effect of surface plasmon polariton-mediated resonances which propagate on a nickel mesh arrayed with 5 micron square holes. Initial results from these spectra indicate that the majority of dust particles contain some degree of organic components, which likely exist in an inorganic matrix. While it currently has not been possible to identify the individual species responsible for the organic signatures in the infrared spectra, it is possible to compare these spectra to various groups to provide an initial degree of characterization. Using the distinguishing peaks from yeast, tar, humic acid, and humic salt spectra, the particles were sorted into groupings. It is believed that these standards may provide a figure of merit for the degree to which the organic components of the particles have decayed.

This work is dedicated to my wife, Lindsey Marie

Acknowledgments

I would like to thank my advisor, Professor James V. Coe, for his instruction, insight, and guidance during my research project. I would also like to thank Marvin Malone and Katie Cilwa for their support and assistance and Matthew McCormack and Michelle Lew for their initial experiments on dust.

Vita

2007.....Upper Arlington High School

2011.....B.S. Chemistry, The Ohio State University

Publications

Katherine E. Cilwa, Matthew C. McCormack, Michelle M. Lew, Christophe I. Robitaille, Lloyd Corwin, Marvin A. Malone, and James V. Coe. "Scatter-Free, Infrared Absorption Spectra of Individual, 3-5 μm, Airborne Dust Particles using Plasmonic Metal Microarrays: A Library of 63 Spectra," Journal of Physical Chemistry, submitted.

Fields of Study

Major Field: Chemistry

Table of Contents

List of Tables

List of Figures

CHAPTER 1 : INTRODUCTION

1.1 Why Dust?

Dust is ubiquitous in our natural environment with global emissions estimated to be on the scale of 1060 to 2070 Tg annually.[1] Dust emissions are known to have significant effects on human health. For instance, exposure to concentrated dust particles was demonstrated to be correlated to increases in heart rate and in blood pressure while simultaneously leading to reduced cardiac contractility in rats predisposed to cardiac stress.[2] Human subjects exposed to concentrated ambient course particles with a mean density of 157 $\mu g/m^3$ were shown to have sizeable changes in cardiac behavior.[3] The average urban concentration of particulate matter, in contrast, is on the order of 30 $\mu g/m^3$. Also, statistically significant correlations have been found between high concentrations of particulate matter and emergency visits for cardiac arrhythmia.[4]

Pulmonary effects due to dust exposure have been noted by several researchers. Exposure to dust particles has been correlated with lung cancer, inflammation, and an induced immune response leading to an increase in the concentration of bronchoalveolar neutrophiles.[5] Experiments on school children in Seoul, Korea found a composition-dependant relationship between the concentration of atmospheric particulate matter and the pulmonary function of the subjects.[6] This provides a motivation for understanding both the concentration of dust as well as the primary components, which is the focus of this investigation.

Particulate matter has also been associated with a rise in all-cause mortality rates. Most notably, the PM_{10} concentration, or the concentration of particulate matter smaller than 10 microns, peaked at levels between 3,830 and 4,460 $\mu g/m^3$ during 1952 in London compared with average values of 30 $\mu g/m^3$ causing an estimated 4,000 to 12,000 fatalities.[7] It has also been suggested that, in general, "a 10-$\mu g\ m^{-3}$ increase in PM_{10} (PM < 10 μm) produces a 0.5% increase in daily mortality."[7]

Studies regarding particulate matter are important because they may aid in understanding dust behavior, creating new standards for acceptable concentrations, and reducing mortality from dangerous exposure.

1.2 The Importance of Organics in Dust

A previous study employing infrared on dust particles in plasmonic mesh has demonstrated that the majority of dust particles contain detectable amount of organic matter.[8] Out of a library of 63 particles, 41 of them were considered organic-containing.[8] It is important to consider the implications of this result and the possibility of differential carcinogenicity between inorganic and organic particulate matter. It has been suggested that the nervous system may be more susceptible to attack by organic particles which appear to have a greater tendency to cross into the olfactory nerve and may pass into the olfactory bulb than inorganic species such as Ir.[9] Industrial exposure to organic particulates, especially carbon black has been shown to cause chronic bronchitis and a 100 percent increase in the incidence of lung cancer.[5] Previous studies have also consistently found a link between inhalation of particulate matter generated from tobacco products and pulmonary disease.[10,11,12] As well, some concern has been expressed regarding inhalation of combustion products from wood smoke and similar sources.[13,14]

While there is a substantial amount of research directed toward the study of organic particulate matter, most studies have investigated this matter as it is emitted from the source rather than in the ambient air. Furthermore, there appears to be an emphasis on the physical characteristics, concentration, and origin of the particles, rather than their chemical composition. Studies which analyze the components of organic dust are primarily characterized by spectroscopic studies of organics extracted into a solvent, failing to account for interactions between the organic and inorganic components.

Obtaining infrared spectra of these particles on plasmonic mesh allows one to determine both organic and inorganic components in particulate matter simultaneously. This is of some importance because it is likely that the presence of organic components may enhance the carcinogenic behavior of inorganic constituents and vice versa. In addition, organic compounds may preferentially associate with certain inorganic species.

CHAPTER 2 : COLLECTION AND PHYSICAL CHARACTERIZATION OF DUST

2.1 Dust Collection Procedures

A piece of nickel mesh with 5 micron square holes, a 12.6 micron hole spacing, and 2 micron thickness was mounted on a piece of aluminum shim stock with a piece of tape, which was then mounted in a plastic filter holder. The assembly is depicted in Figure 2.1.

Figure 2.1: Dust Filter Holder and Mesh Mounted on Aluminum Shim Stock

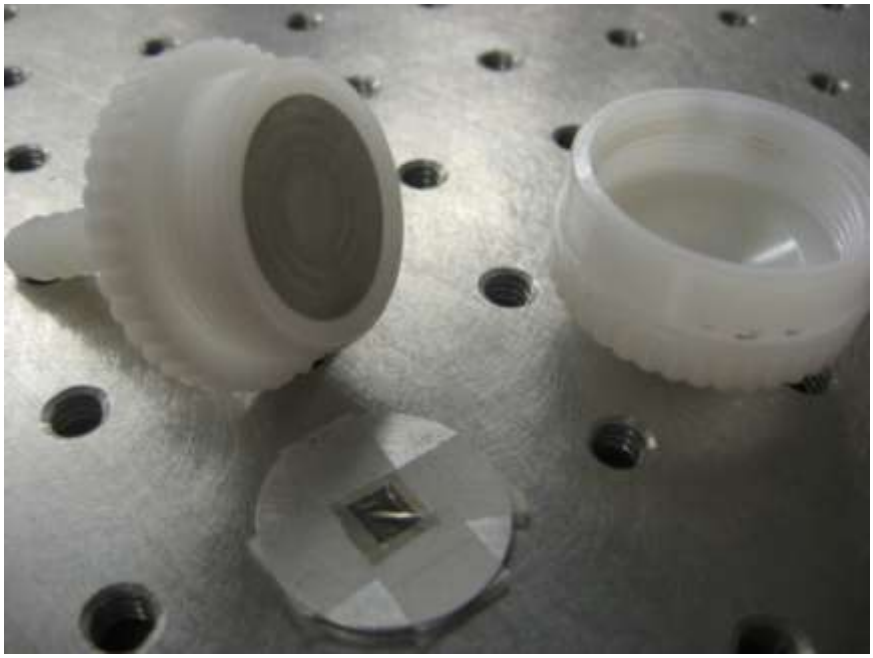

The assembly was attached to an air flow meter and a Quick Take 30 mechanical air pump with plastic tubing. Pumping speed was adjusted using the flow meter to a speed of 5 L/min and dust was collected in this manner for 18 hours. The sample produced from this collection was labeled as “C2.” A figure depicting the collection apparatus may be found below as Figure 2.2.

Figure 2.2: Collection Apparatus

Spectra were obtained from the sample, “C2,” using an FTIR microscope. Results from this experiment may be found in Chapter 3.

A slightly different collection procedure was performed for an experiment relating the mass of dust collected to the time of collection. Due to the constraints of the weighting system, an electrobalance, it was not possible to mount the mesh directly to the shim

stock because due to the large additional mass added by the aluminum sheet. It was necessary to weigh the mesh independent of the shim stock. The mesh was mounted in a piece of folded brass sheet metal as shown in Figure 2.3.

Figure 2.3: Mesh Mounting for Dust Mass versus Time Experiment

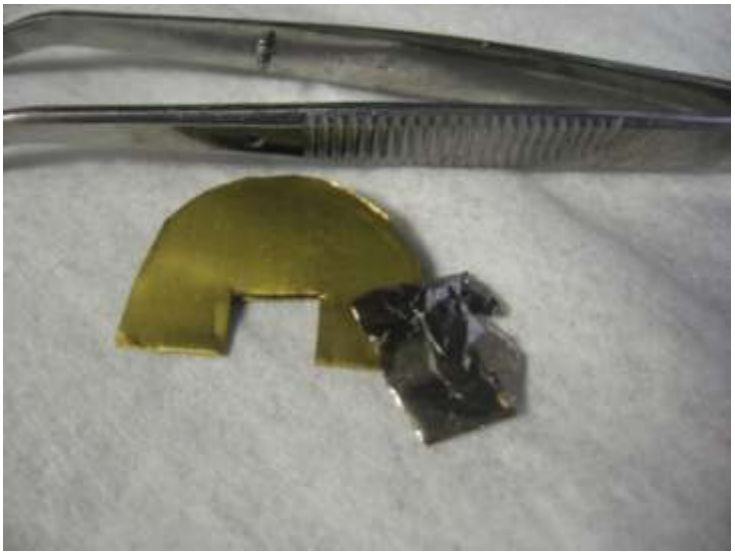

The mounting was inserted into the plastic filter holder with a piece of paper blocking the open paths of air flow except for directly through the mesh. This design allowed for removal of the mesh sample for each mass reading which was performed on a CAHN electrobalance as depicted in Figure 2.4. Since the mass of dust collected at each interval is on the order of micrograms, it is not possible to perform this experiment on a standard analytical balance, which only provides an accuracy of ± 0.1 mg. This accuracy would not register a change in mass even until the collection times were on the order of 2 hours. In contrast, the CAHN electrobalance has an accuracy of ± 0.1 μg and would theoretically be capable of measuring mass changes on a minute-by-minute basis.

Figure 2.4: CAHN electrobalance

Collecting dust following this procedure yields information regarding the concentration of dust in the local atmosphere. Further discussion of this experiment may be found in Section 2.2 below.

2.2 Dust Mass Collected Versus Time

An experiment was performed to determine the concentration of dust in the laboratory atmosphere. The density of laboratory dust was assessed by pumping air through a piece of metal mesh at a known velocity and taking the mass of the sample periodically. The results obtained from this experiment are shown in Table 2.1.

Table 2.1: Dust Mass versus Collection Time

Time (min)	Mass (mg)
0	0.0000
20	0.0140
40	0.0225
61	0.0335
81	0.0440

A linear least-squares fit performed on this data yields a slope with a value of 5.53×10^{-4} mg/min. This value, *m*, may be divided by the flow rate, *R*, of 16.5 L/min to determine the density of particulate matter in the laboratory air.

$$\rho = \frac{m}{R}$$

$$\rho = \frac{(5.5 \pm 1.4) \times 10^{-4}\ \text{mg/min}}{16.5\ \text{L/min}} = (3.35 \pm 0.08) \times 10^{-5}\text{mg/L}$$

$$\rho = 33.5 \pm 0.8\ \mu\text{g/m}^3$$

The density obtained from this experiment is in agreement with the expected concentration of 30 μg/m^3. The experiment was repeated by another investigator and yielded a density of particulate matter corresponding to a value of 43.3 ± 1.5 μg/m^3. A plot of the representative data, along with the least-squares trendlines, is shown in Figure 2.5 and Figure 2.6.

Figure 2.5: Dust Mass versus Collection Time

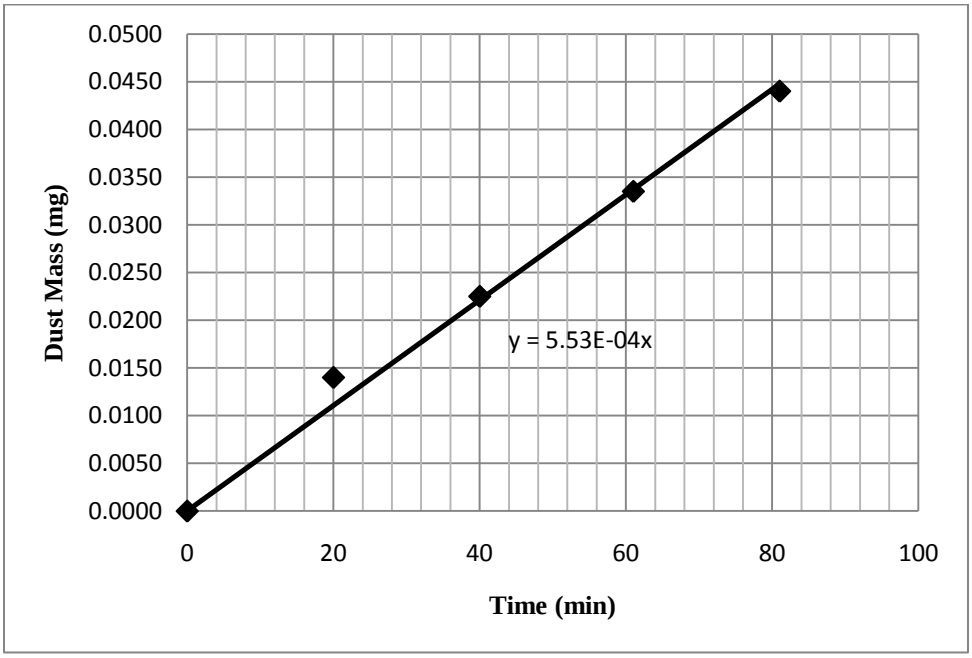

Figure 2.6: Dust Mass versus Collection Time

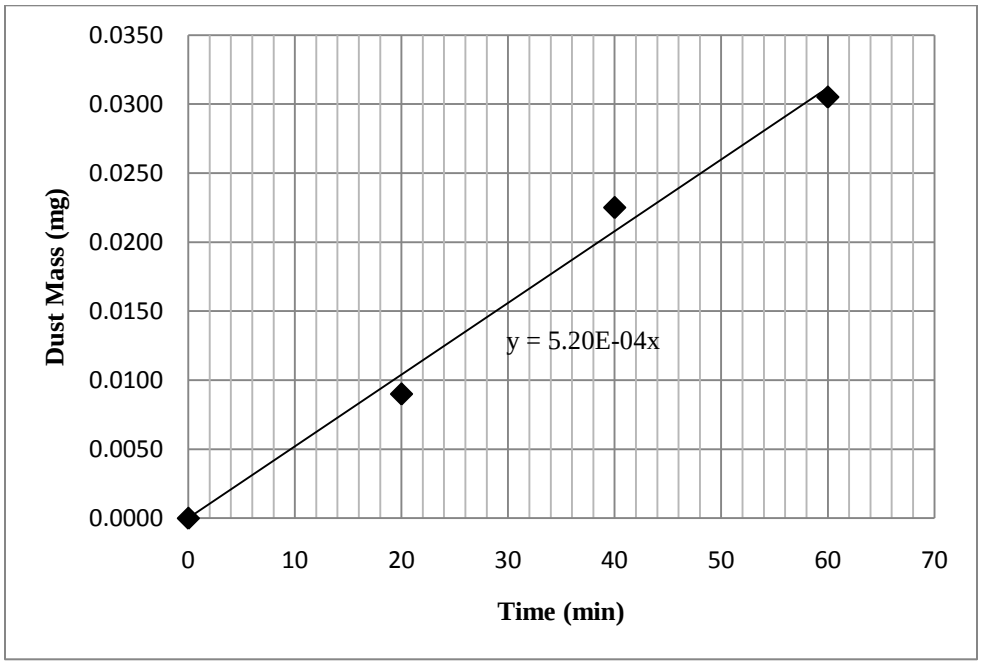

2.3 Particle Counts

For the purposes of determining the temporally-dependant aspects of particulate matter concentrations, an experiment was performed whereby the number of dust particles of a given size could be counted as they are pumped across the path of a laser. A Kanomax Handheld Laser Particle Counter Model 3887, capable of counting 0.3, 0.5, and 5.0 μm particles, was employed to characterize this behavior. Each size particle was measured simultaneously over a period of time with step sizes of 1.0 minutes. It was then possible to take the averages and standard deviations of the 1.0 minute particle counts to determine both the relative concentration and variation in concentration for each species. The data from each particle count may be found in Figure 2.7 through Figure 2.18. A table showing the counts, standard deviations, percent relative standard deviations, and standard deviations relative to the 5.0 μm particle counts may be found in Table 2.2. Since the 5.0 μm particle counts were the most variable of the three sizes, a comparison of each particle size's relative standard deviation to the standard deviation of this size may be utilized to standardize variations between all species. Using this method, it was found that the 0.3 and 0.5 micron particles only had variabilities on the order of 10 and 25 % when compared with the variations observed in the 5.0 micron particles.

Table 2.2: Particle Count Statistics

	Trial 1			Trial 2			Trial 3			Trial 4		
	0.3 μm	0.5 μm	5.0 μm	0.3 μm	0.5 μm	5.0 μm	0.3 μm	0.5 μm	5.0 μm	0.3 μm	0.5 μm	5.0 μm
Average Count	71000	5900	24	81000	10000	46	64000	4600	28	38000	3000	23
Standard Deviation	2500	300	13	8000	3000	50	13000	1600	40	3000	800	16
Percent Relative Standard Deviation	3.50	5.59	52.52	9.84	29.66	109.76	20.50	34.84	131.48	8.05	25.59	69.67
Standard Deviation Relative to 5.0 μm	6.67	10.64	100.00	8.96	27.03	100.00	15.59	26.50	100.00	11.56	36.74	100.00

While the presence of 0.3 and 0.5 μm particles appears to constitute an overwhelming majority, one must realize that the absolute number of particles may not be meaningful without considering the volume delivered by each species. In this size range, all particles are able to establish a long-term presence in the lungs with relative ease. However, dust on the order of 5 microns is capable of carrying a much larger carcinogenic payload than its smaller counterparts. The volume of each species and volume fraction relative to the 5 micron species are listed in Table 2.3.

Table 2.3: Particle Volumes and Volume Fractions

Particle Size	0.3 μm	0.5 μm	5.0 μm
Volume (μm^3)	0.014	0.065	65
Volume Fraction	0.00022	0.0010	1.0

By multiplying each particle count by the relative volume fraction, it is possible to obtain each count adjusted to the 5 μm particle size. In essence, this procedure will yield the counts that would be recorded if all the smaller particles were aggregated into 5 micron species. These numbers allow one to more readily compare the masses and possible carcinogenic payloads contained by each particle size. The "adjusted" counts averaged from all four trials are listed in Table 2.4

Table 2.4: Volume Adjusted Particle Counts

Particle Size	0.3 μm	0.5 μm	5.0 μm
5 Micron Adjusted Particle Counts	13.76	5.96	30.48

The above table suggests that, after adjusting for the volume, 5 micron particles have an important contribution to mass density in the atmosphere. Since these species are have the largest mass concentration in air as well as the greatest potential for carrying large carcinogenic payloads, they are the most concerning of the three sizes in regard to their toxicity.

Following the above logic, one might assume that a presence of particles larger than 5 microns, due to their greater volume, would be even more alarming in regards to human health. However, these particles have difficulty deeply penetrating the lungs. Since 5 micron particles strike the right balance between the size necessary for lung penetration, concentration, and carcinogenic load, they may represent an important size for investigation.

Figure 2.7: Trial 1, 0.3 µm Particle Counts versus Time

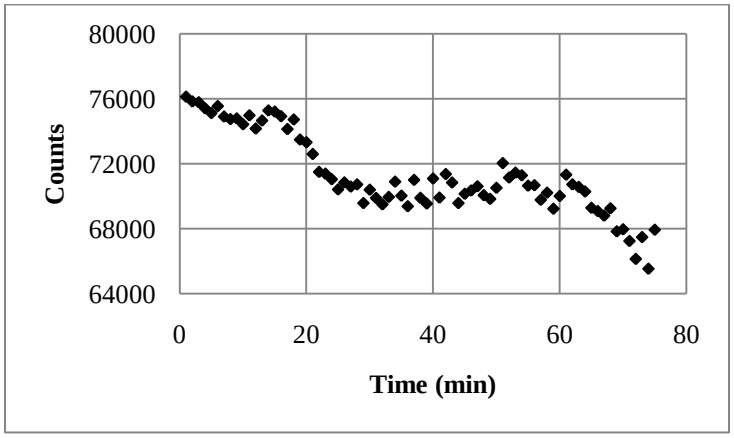

Figure 2.8: Trial 1, 0.5 µm Particle Counts versus Time

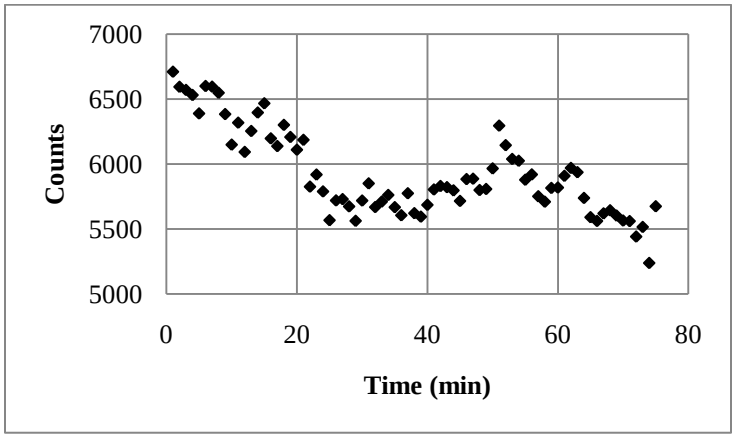

Figure 2.9: Trial 1, 5.0 µm Particle Counts versus Time

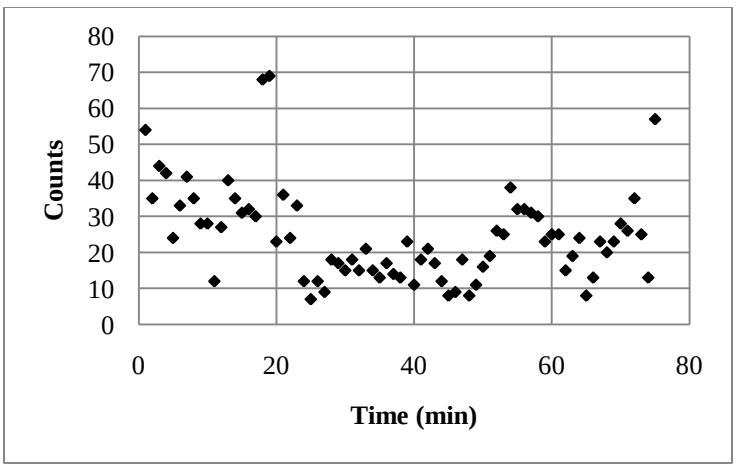

Figure 2.10: Trial 2, 0.3 µm Particle Counts versus Time

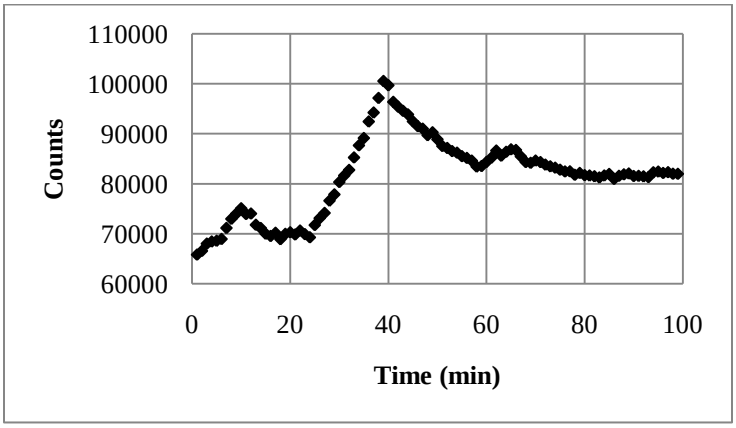

Figure 2.11: Trial 2, 0.5 µm Particle Counts versus Time

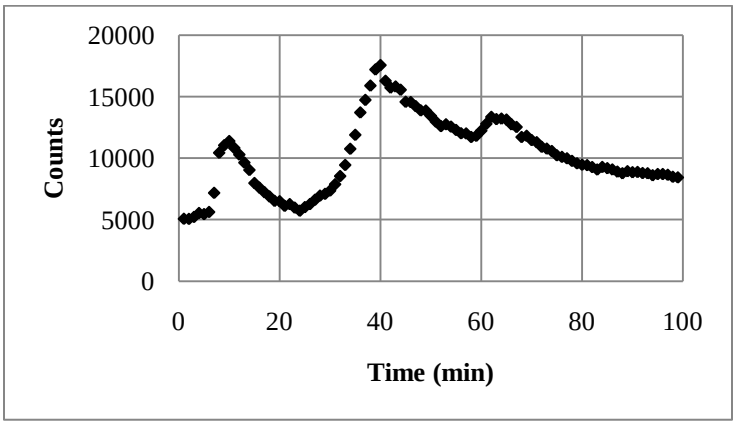

Figure 2.12: Trial 2, 5.0 µm Particle Counts versus Time

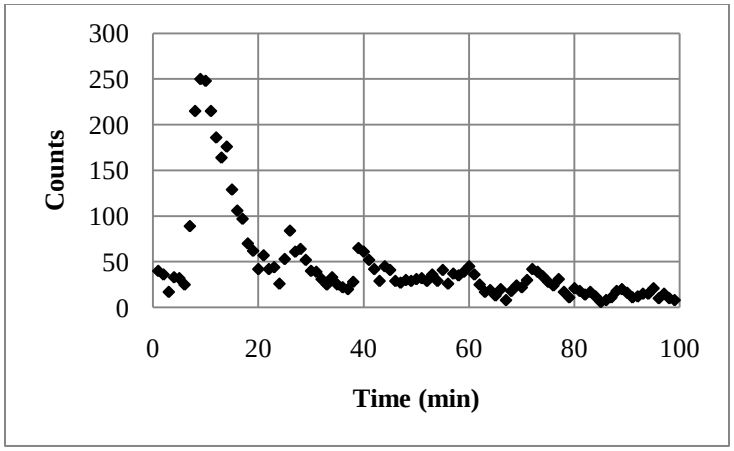

Figure 2.13: Trial 3, 0.3 µm Particle Counts versus Time

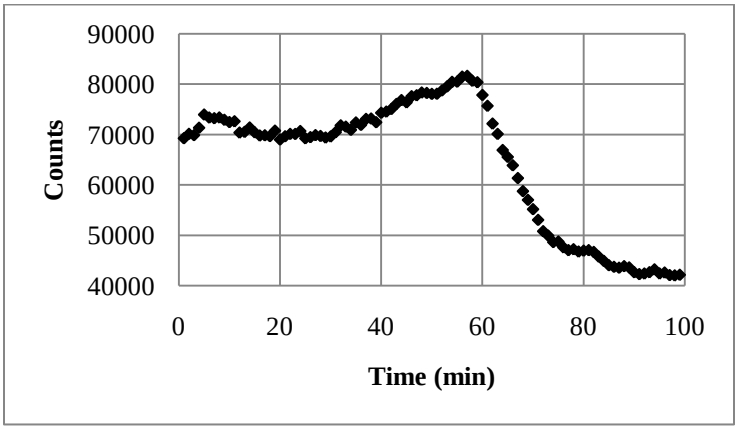

Figure 2.14: Trial 3, 0.5 µm Particle Counts versus Time

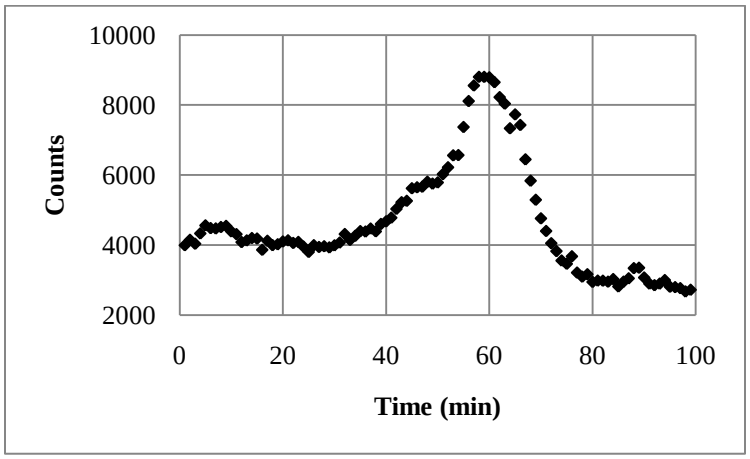

Figure 2.15: Trial 3, 5.0 µm Particle Counts versus Time

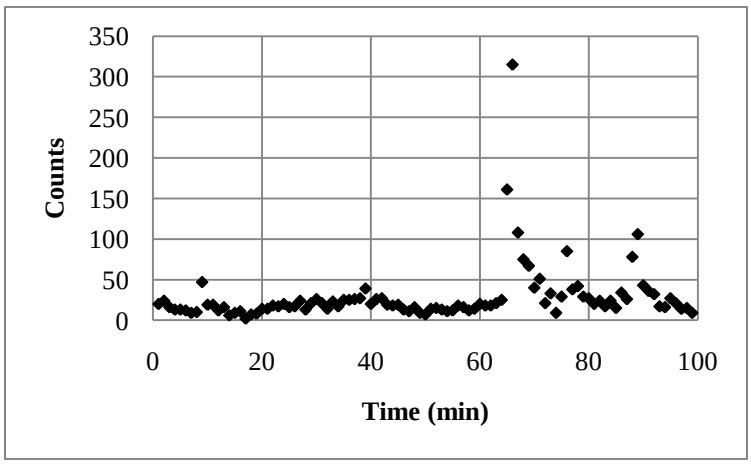

Figure 2.16: Trial 4, 0.3 µm Particle Counts versus Time

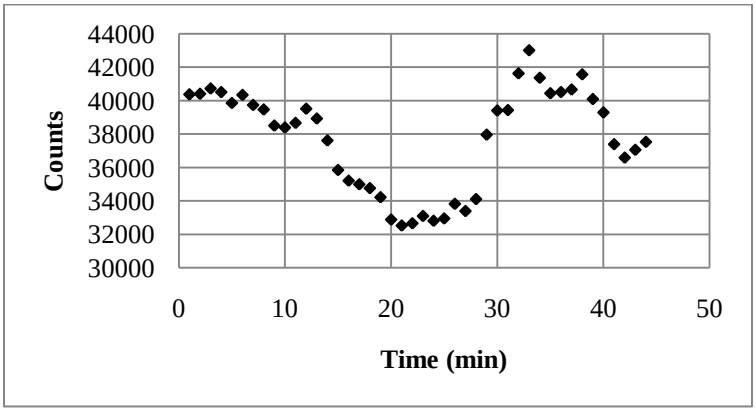

Figure 2.17: Trial 4, 0.5 µm Particle Counts versus Time

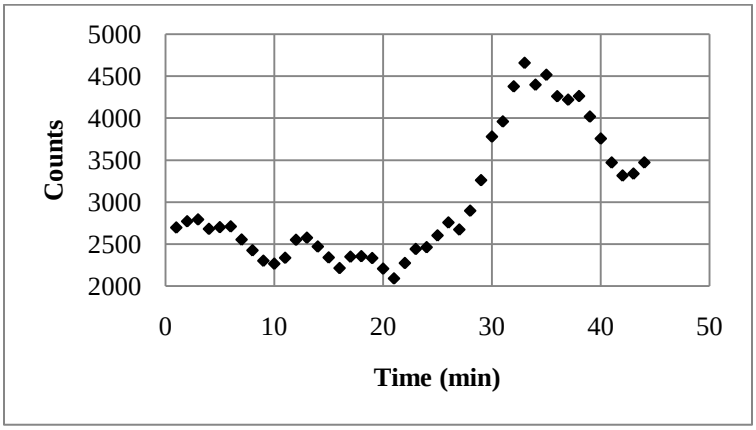

Figure 2.18: Trial 4, 5.0 µm Particle Counts versus Time

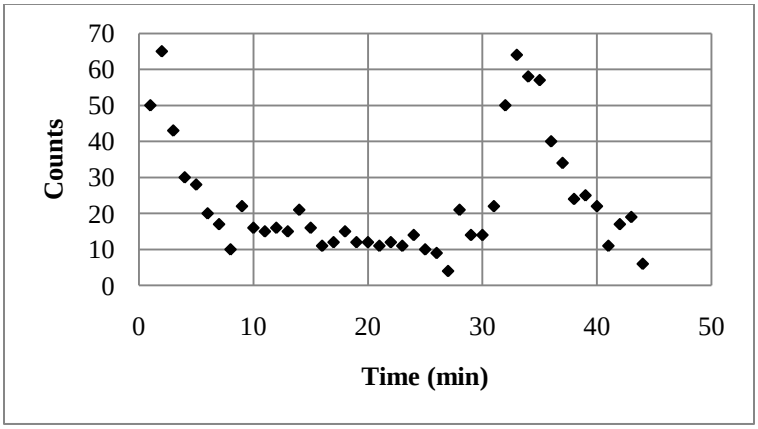

CHAPTER 3 : ORGANIC COMPONENTS IN DUST

3.1 Scatter-Free Spectra of Individual Dust Particles with Organics

Dust particles collected for this experiment are on the order of 5 μm in size and, due to their sizes being similar to the wavelength of infrared light, scatter light effectively. This is also known as Mie scattering. Scattering is of such great intensity for these particles that it is difficult to obtain quantitative or sometimes even qualitative spectra of these species. However, when these dust particles are captured within the holes of a metallic mesh, interactions of infrared light with the array will generate surface plasmon polaritons, which propagate along the mesh surface and couple through the holes without scattering while interacting favorably with species contained within the square holes to produce standard absorption spectra.[8] The differences in spectra obtained with particulate matter on a surface versus in metal mesh are shown in Figure 3.1.

Figure 3.1: ZnSe Scattering Spectra versus Plasmonic Mesh Absorption Spectra

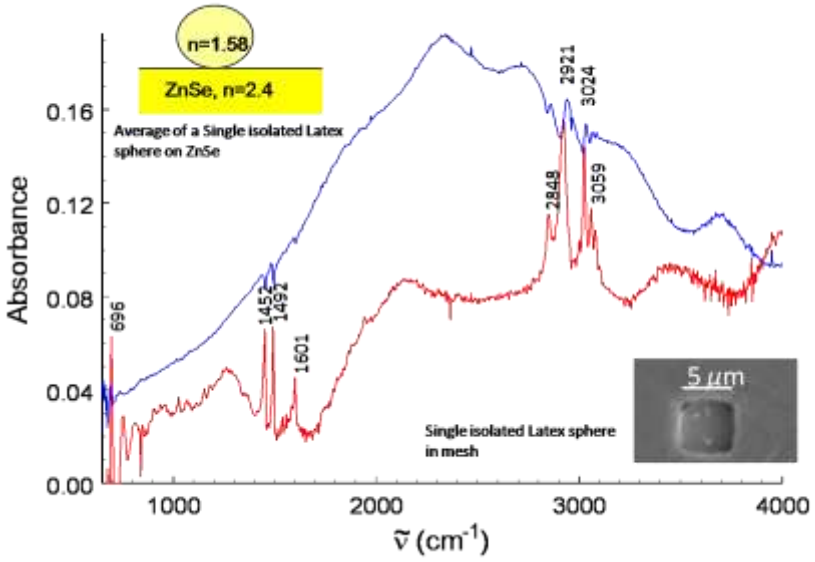

Scatter-free spectra such as in Figure 3.1 above have been collected for 63 dust particles on sample “C2” and are labeled d1-d63. See Reference 8 for a discussion of the inorganic components of these particles.

3.2 Decomposition of Live Materials on Airborne Dust Particles

Organic matter has a significant presence in dust collected on "C2" and is represented in 41 out of 63 spectra. Two of these particles have a spectra characteristic of small molecule organic species and likely originate from a nearby university chemistry laboratory. The remaining particles have spectra which more closely resemble living matter. Thus, these spectra may represent a continuum of the decay of living matter. To sort the particles into this continuum of decay, they were compared with defining species along the continuum with yeast representing living or recently living material and petroleum representing the most decayed matter. Intermediate species in this decay process include tar, humic acid, and humic salt. It should be noted that humic acid or salt is typically representative of the short-term end-point of organic decay on the surface of the earth, while petroleum-like species represent material that has had a opportunity to decay on geological time scales.

The spectrum of recently living or "yeast-like" particles has been established by previous research.[15] Defining features of these particles include aliphatic, carbonyl, amide I, amide II, and amide III peaks at approximately 2927, 1730, 1652, 1544 and 1436 cm^{-1}, respectively. A defining spectrum for recently living particles may be found below in Figure 3.2. It is believed that all recently living material should contain the above features which are the result of aliphatic chains, proteins, phospholipids, RNA, sugars, et cetera. Thus, the spectrum obtained from a yeast cell may provide an appropriate standard for determining whether matter is living or was recently living.

Next in the continuum of decay is tar. Spectra of tar were obtained using two methods. The first method was to draw air through a sample of mesh at 5 L/min while exposing the sample holder entrance aperture directly to smoke produced from a burning cigarette. Unfortunately, the particles captured in this manner did not retain their shape and smeared across the mesh surface, making it impossible to obtain single particle spectra. However, the average spectra from a 200 micron by 200 micron area provided some insight into the principle features of tar. Aliphatic, carbonyl, and amide peaks are visualized at approximately 2923, 1770, and 1686 cm^{-1}, respectively. Additionally, there is universally a peak observed at ~ 810 cm^{-1} whose vibrational source is of unknown origin.

A second method was also utilized to obtain spectra for tar in a manner that would allow for single particle analysis. Dust was collected from a bookshelf in Evans Laboratory room 0027 and was placed in a plastic bag. Smoke produced from a cigarette was exhaled into this bag as it was shaken to expose individual particles to the fumes, thereby possibly coating the particles with a thin layer of tar. This sample was collected by placing the sample directly on the mesh and drawing the particles into the holes with an air pump speed of ~ 5 L/min and a collection time of approximately 1 minute. Spectra were collected of individual particles and demonstrated similar results to those found for the previous method. Again, there are peaks at 2916, 1716, and 1653 cm^{-1}, for the aliphatic, carbonyl, and amide functionalities, respectively. Amide II and amide III peaks were

sometimes visualized, but with significantly reduced intensity when compared with the recently living group. A defining spectrum for tar is shown in Figure 3.3.

Humic acid and humic salt were obtained for the purpose of characterizing the next level in the decay continuum. Samples arrived in crystalline form and were crushed with a mortar and pestle for approximately 10 minutes to produce particles on the order of 5 microns in size. A sample of the solid powder was placed directly on the mesh and particles were drawn through using a flow rate of 5 L/min and a collection time of approximately 30 seconds. The humic acid and humic salt particles were collected on two separate samples of mesh. Spectra were then obtained for the two species and it was found that there were no significant differences between the peaks of the humic acid and humic salt samples. Further analysis suggested that the humic acid sample was primarily comprised of humic salt and, thus, it was difficult to determine the peaks associated with the acid compound. Humic salt has two features which may be used for its identification. These peaks are relatively strong in intensity when compared with the aliphatic peak and appear at approximately 1570 and 1370 $cm^{-1}$with a tendency to shift slightly depending on the matrix. These peaks have been labeled “Humic I” for the former and “Humic II” for the latter to distinguish them from other features. The spectra of this compound have a notable absence of the carbonyl stretch. However, some of the spectra analyzed appear to have the “Humic I” and “Humic II” peaks in addition to a carbonyl peak. It has been assumed that these structures appearing together are indicative of humic acid and salt.

Defining spectra for humic acid and humic salt may be referenced in Figure 3.4 and Figure 3.5, respectively.

Particles which contain no identifiable organic signatures other than an aliphatic stretch are placed into the petroleum or oil-like group. This assignment is based on the fact that petroleum primarily consists of aliphatic or aromatic functionalities. The defining spectrum for this group may be found in Figure 3.6.

Figure 3.2: Recently Living or "Yeast-Like" Defining Spectrum (d21)

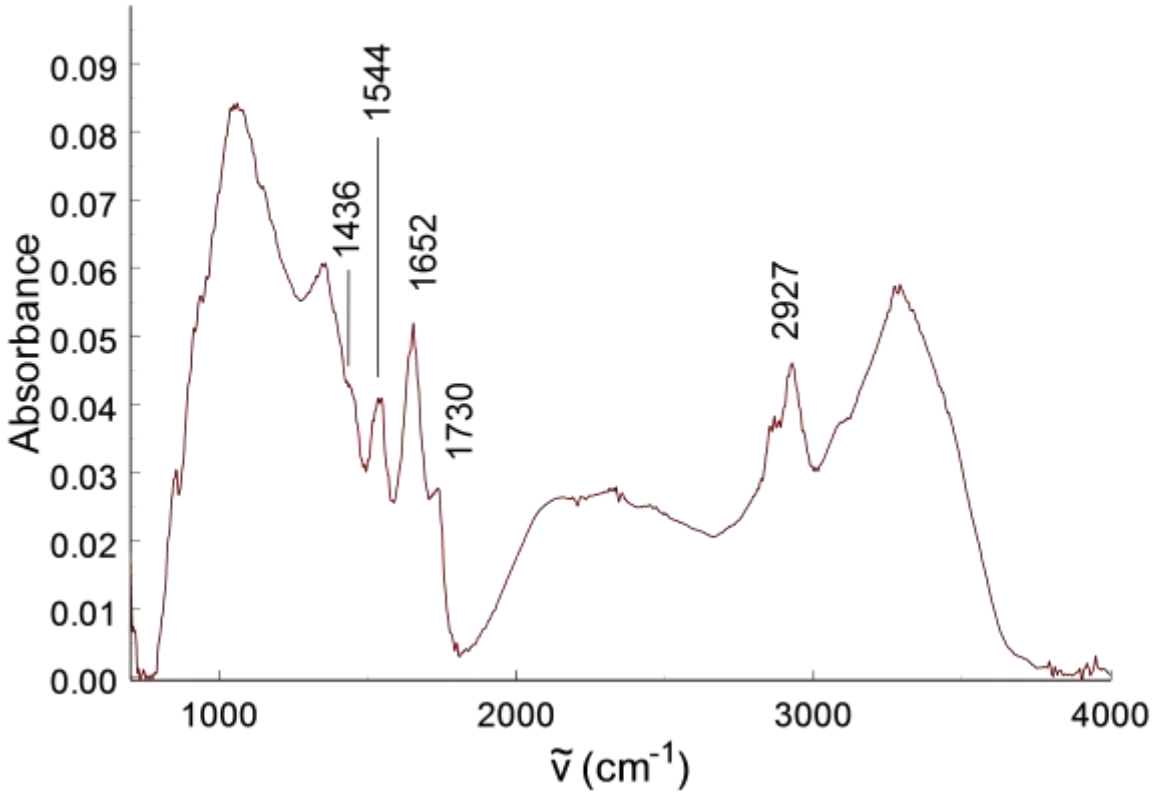

Figure 3.3: Tar Defining Spectrum (d31)

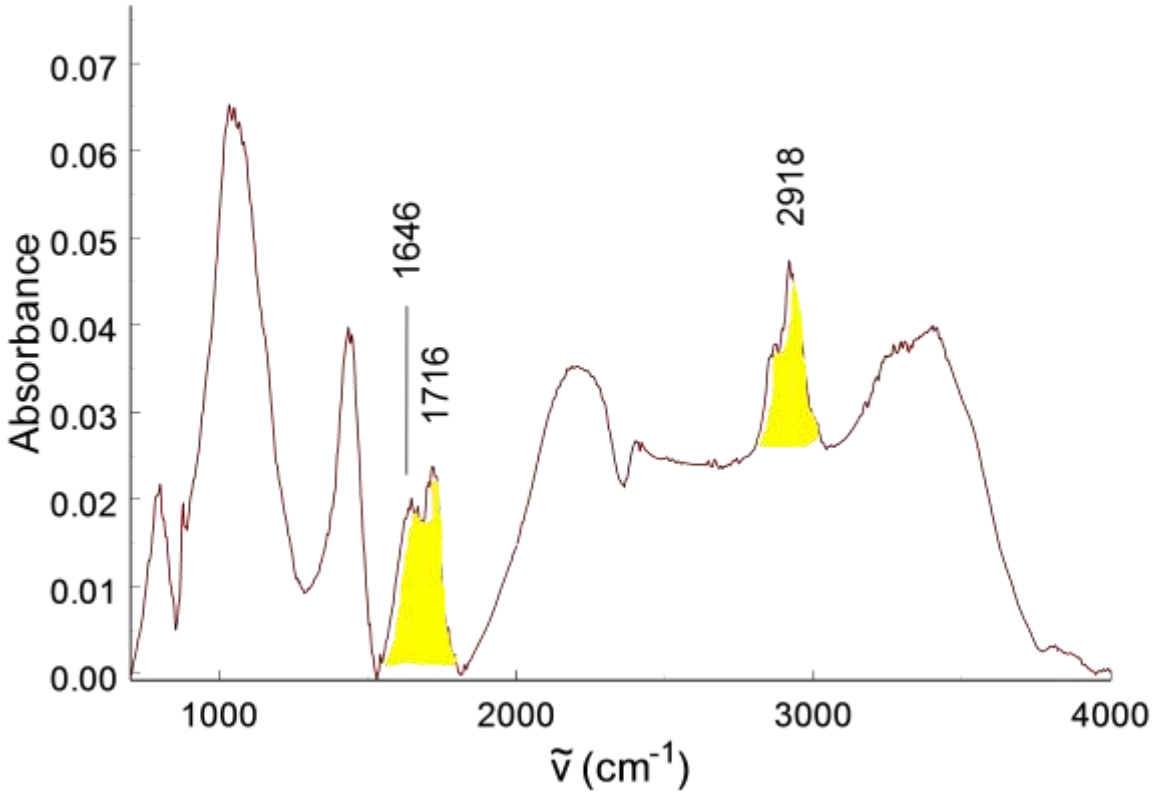

Figure 3.4: Humic Acid Defining Spectrum (d8)

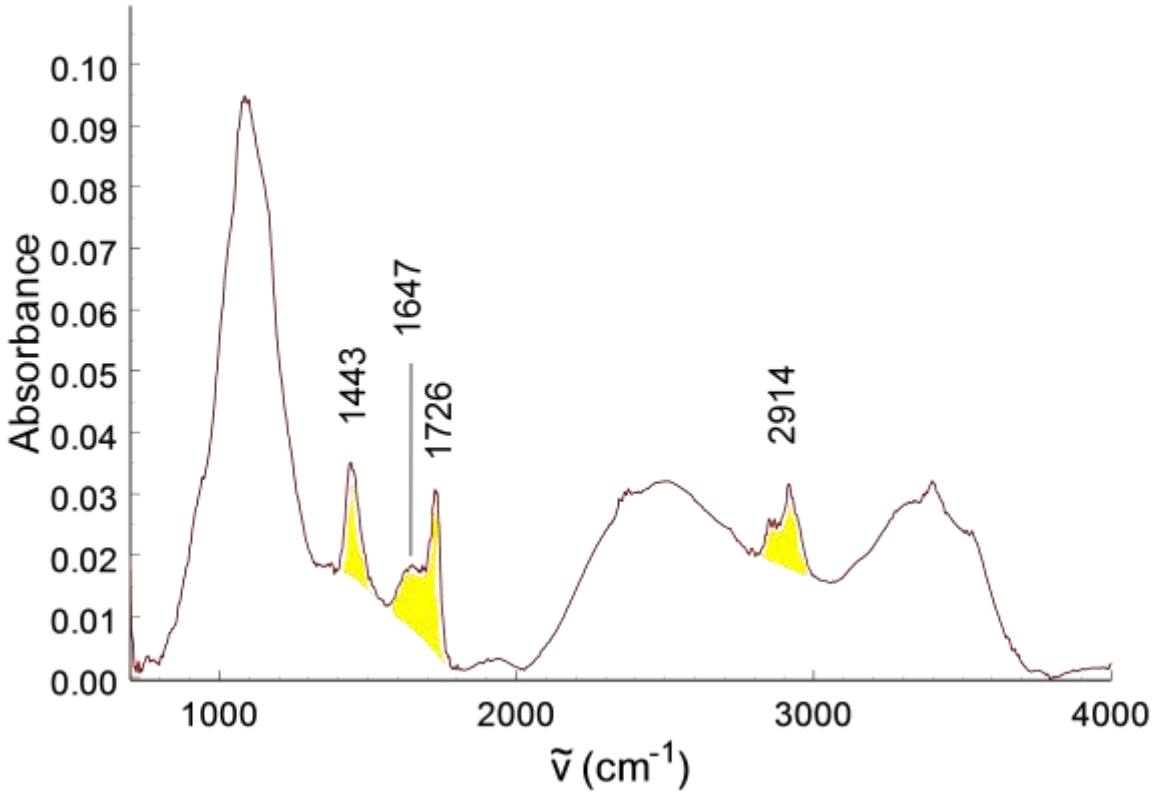

Figure 3.5: Humic Salt Defining Spectrum (d57)

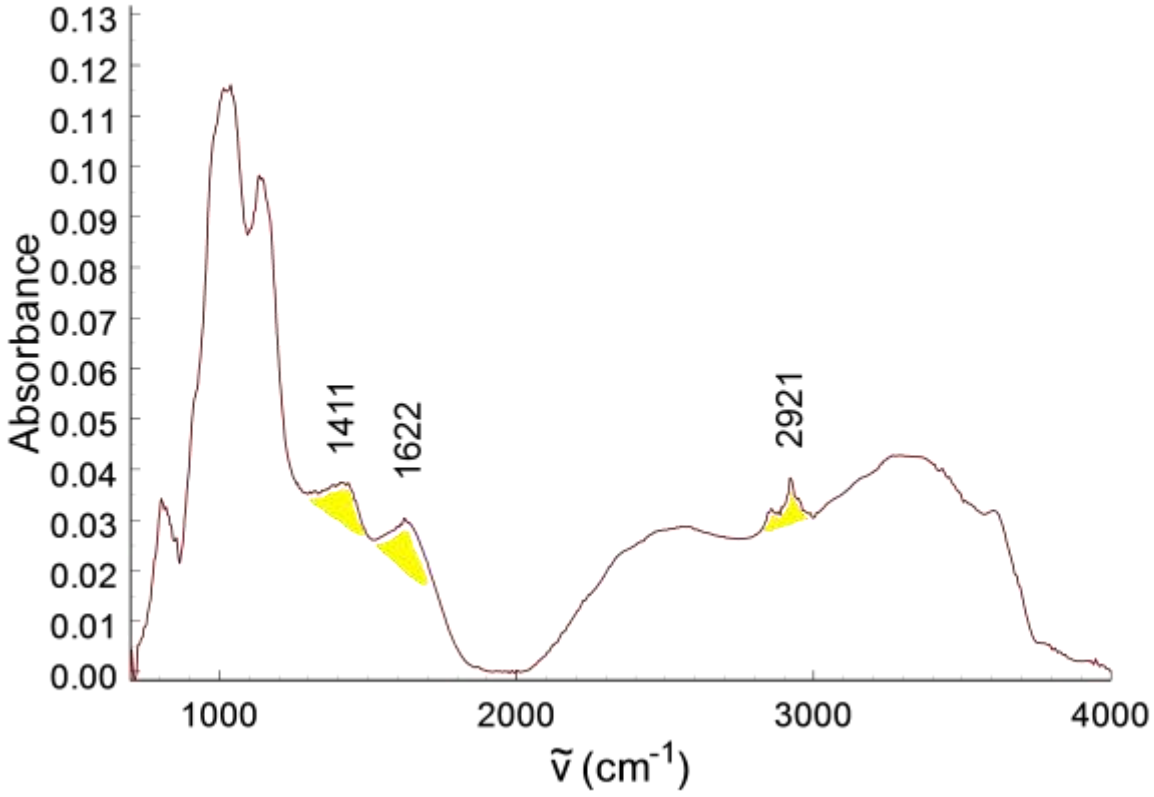

Figure 3.6: Petroleum or "Oil-Like" Defining Spectrum (d63)

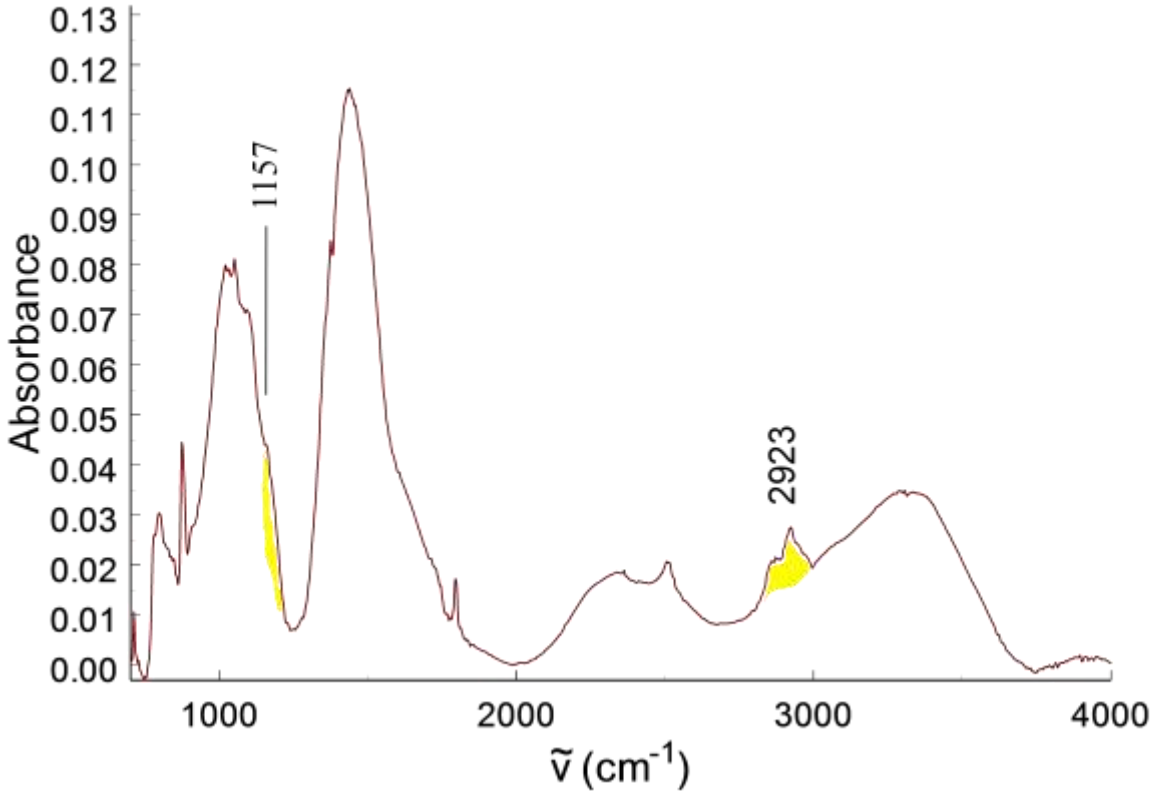

Using the criteria established above, the 63 individual particles were categorized according to their position on the decay continuum. Groupings of these particles including peak areas for all defining peaks may be found in Table 3.1 through Table 3.5. Spectra of these groupings are in Figure 3.7 through Figure 3.11. The areas were obtained by taking baselines underneath each peak. Peak areas should not be taken as absolute because baselines were placed at peak valleys in the case of non-resolved peaks, causing substantial underestimates for the areas of certain peaks. Fitting the peaks with Gaussian functions should produce more quantitatively accurate results.

Table 3.1: Recently Living or Yeast-Like Particles (units A·cm^{-1})

Particle Identifier	Inorganic Components	Aliphatic	Carbonyl	Amide I	Amide II	Amide III
d5	Clay	1.424	0.0236	1.5873	0.2603	0.2783
d21	Clay	1.8619	0.319	1.364	0.5968	0.1104
d28	Clay	2.1682	0.4345	1.6605	0.678	0.1384
d62	Clay	0.7256	0.132	1.3165	0.2477	0.3162

Table 3.2: Tar-Like Particles (units A·cm^{-1})

Particle Identifier	Inorganic Components	Aliphatic	Carbonyl	Amide I
d1	Clay, Gypsum	1.0807	None	0.0122
d16	Clay	0.7335	0.111	0.2116
d31	Quartz, Clay	2.3532	0.5359	0.5609
d33	Clay	1.227	0.1613	0.2869
d37	Clay	3.294	0.7493	0.7929
d45	Clay, Quartz	2.2647	0.8658	0.1948
d53	Clay	0.4475	0.146	0.0682
d55	Gypsum, Clay	1.5304	0.3634	0.3898
d58	Clay, Gypsum, Dolomite	1.9222	0.4549	0.1771
d60	Clay	2.367	0.1919	0.9372

Table 3.3: Humic Acid-Like Particles (units A·cm^{-1})

Particle Identifier	Inorganic Components	Aliphatic	Carbonyl	Humic I	Humic II
d6	Clay, Gypsum, Quartz	1.0196	0.2682	0.1585	1.1189
d12	Gypsum	3.5851	0.1202	0.8628	overlap
d14	Quartz	1.6176	0.2256	0.6753	overlap
d20	Clay	1.6987	0.5267	0.1273	0.3376
d27	Clay, Quartz	1.6529	0.6466	0.1072	overlap
d34	Clay	1.2111	0.3475	0.1768	0.3164
d39	Clay	0.6693	0.1249	0.4021	1.0705
d40	Clay, Quartz	1.1783	0.1342	0.0425	1.5304
d47	Clay	1.1662	0.6286	0.0869	0.4994
d54	Gypsum	1.3671	0.8295	0.2642	2.8440

Table 3.4: Humic Salt-Like Particles (units A·cm^{-1})

Particle Identifier	Inorganic Components	Aliphatic	Humic I	Humic 2
d2	Gypsum	0.2367	1.7145	0.2314
d11	Clay, Quartz	0.4000	0.6604	0.7565
d23	Clay	0.7958	1.1397	0.7342
d32	Gypsum	0.3188	1.1068	0.4379
d35	Clay	0.7257	1.8974	2.3573
d46	Clay, Quartz	1.0543	2.3180	0.7049
d50	Clay, Limestone, Quartz	2.0985	1.4977	6.3975
d57	Clay, Quartz	0.6481	1.9187	0.7785
d61	Gypsum	0.9763	0.6845	1.3970

Table 3.5: Petroleum or Oil-Like Particles (units A·cm^{-1})

Particle Identifier	Inorganic Components	Aliphatic
d15	Gypsum, Quartz	0.7691
d63	Limestone, Quartz	1.0808

Figure 3.7: Recently Living Particle Spectra

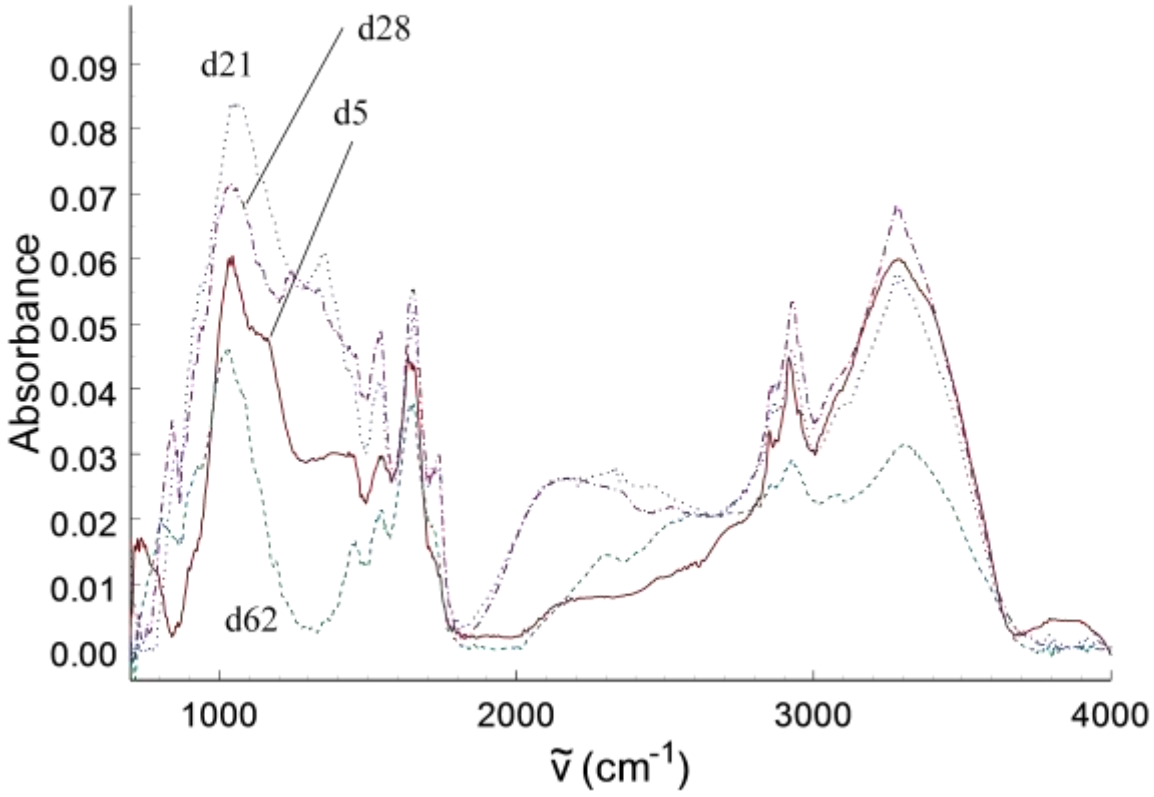

Figure 3.8: Tar-Like Particle Spectra

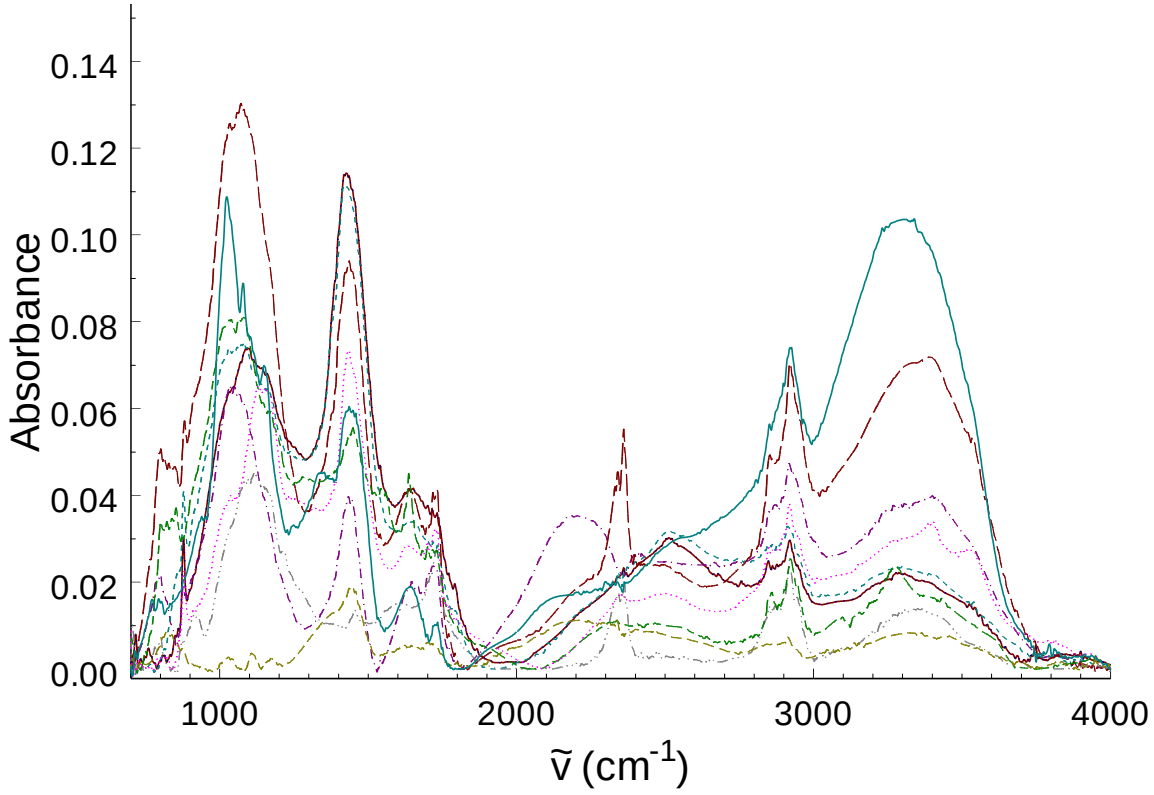

Figure 3.9: Humic Acid-Like Particle Spectra

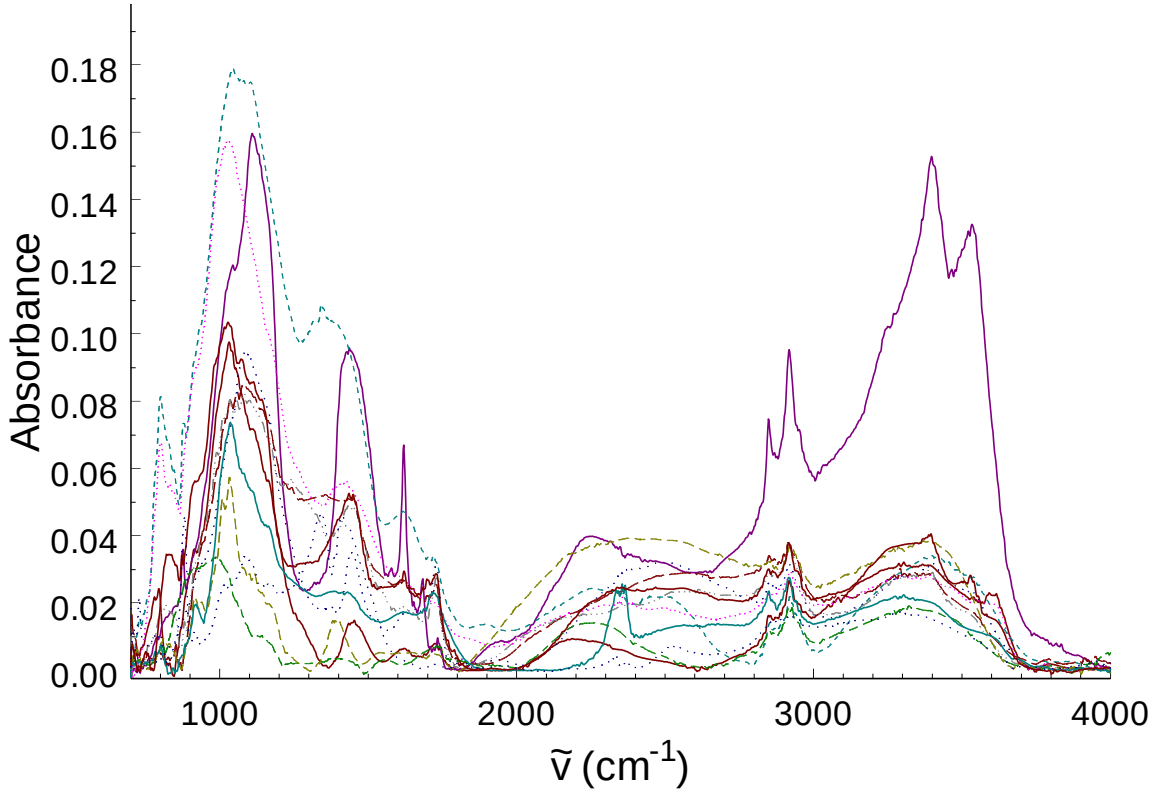

Figure 3.10: Humic Salt–Like Particle Spectra

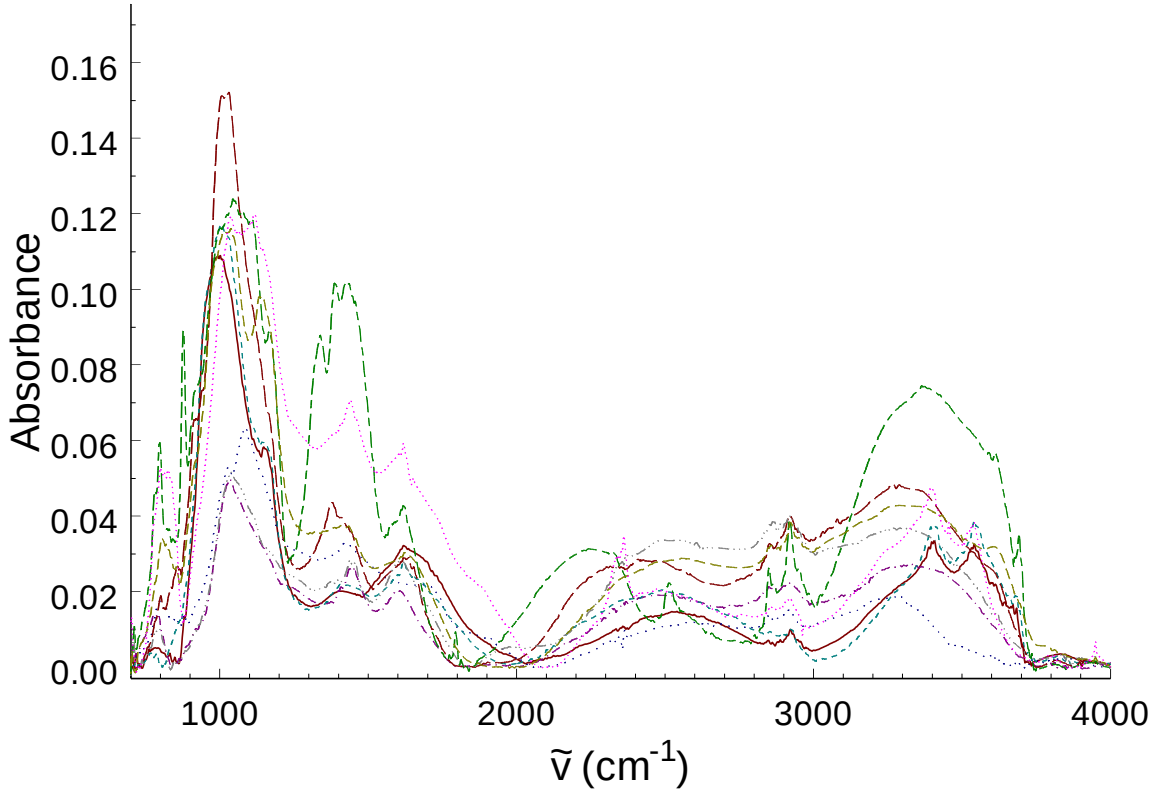

Figure 3.11: Petroleum-Like Particle Spectra

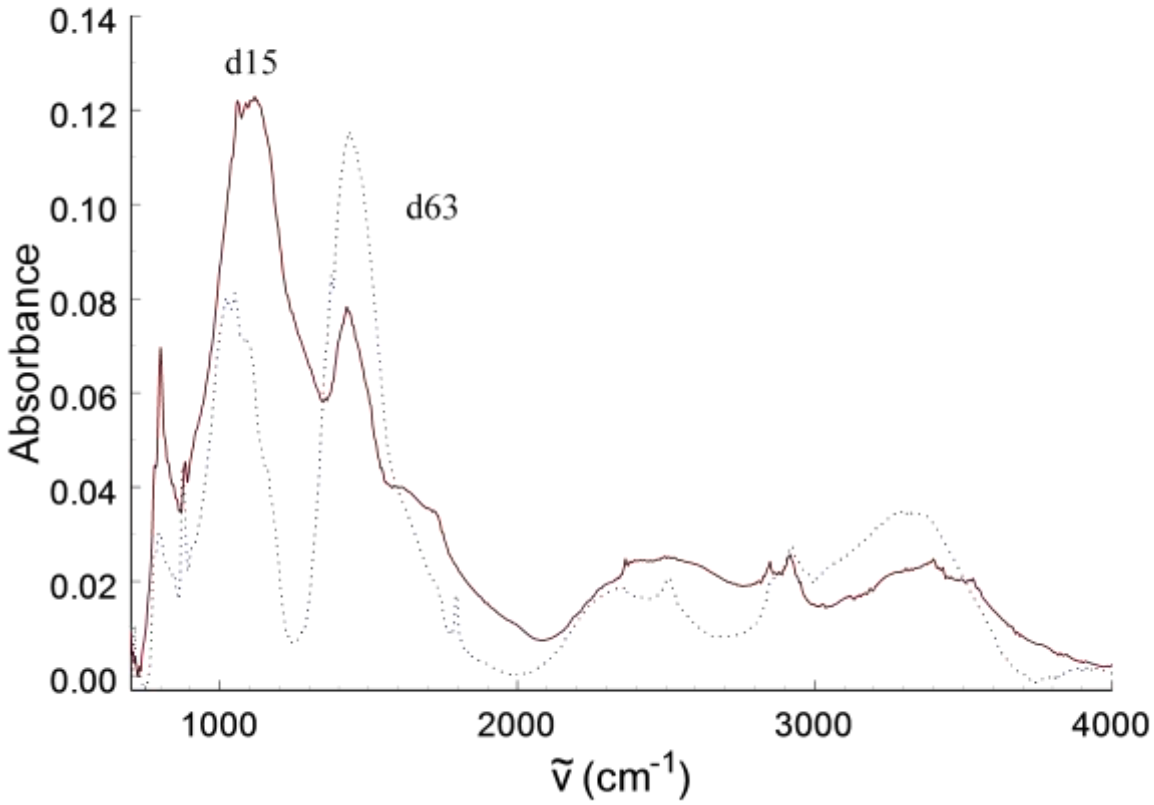

CHAPTER 4 : CONCLUSIONS

It was found that there is a strong presence of more decayed organic matter when compared with recently living matter. Most of the particles studied fall either into the humic acid or humic salt group, suggesting that the majority of dust in the air has organic components which originate from material which is relatively advanced in its decay process. Only two particles were found in the category of petroleum or oil-like which may indicate that the mechanisms of oil naturally rising to the earth's surface may not be sufficient to have an impact on dust composition, oil may not associate strongly with particulate matter, or that such compounds may not have enough thermodynamic stability to support their existence in the earth's atmosphere at long time scales.

The results from the dust mass versus time experiment indicate that the concentration of particulate matter on the university campus is representative of the average urban concentration.

The experiments with particle counts show that the presence of 5 micron sized particles is of a large concern to human health do to their large concentration by volume and the potential for delivering relatively greater carcinogenic payloads. The independent and highly fluctuating behavior of these particle's concentration in air suggest that it may be necessary to design more efficient filtration systems to reduce physiological harm.

This technique of taking spectra of individual particles on plasmonic mesh has allowed for resolution of organic peaks other than the aliphatic peak. Bulk spectra show the hydrocarbon stretching peak, but other organic peaks are typically obscured by the averaging of mineral components. The methodology utilized in this thesis for analysis of particulate matter will eventually lead to enhanced characterization of the organic species.

REFERENCES

[1] Hoffmann, C.; Funk, R.; Sommer, M.; Li, Yong. Temporal Variations in PM10 and Particle Size Distribution during Asian Dust Storms in Inner Mongolia. *Atmospheric Environment*. **2008**, 42, 8422-8431.

[2] Chang, C.; et al. Effects of Concentrated Ambient Particles on Heart Rate, Blood Pressure, and Cardiac Contractility in Spontaneously Hypertensive Rats. *Inhalation Toxicology*. **2004**, 16, 421-429.

[3] Gong, H.; et al. Altered Heart-Rate Variability in Asthmatic and Healthy Volunteers Exposed to Concentrated Ambient Coarse Particles. *Inhalation Toxicology*. **2004**, 16, 335-343.

[4] Tsai, S-S.; Chiu, H-F.; Wu, T-N.; Yang, C-Y. Air Pollution and Emergency Room Visits for Cardiac Arrhythmia in a Subtropical City: Taipei, Taiwan. *Inhalation Toxicology*. **2009**, 21 (113), 1113-1118.

[5] Roller, M. Carcinogenicity of Inhaled Nanoparticles. *Inhalation Toxicology*. **2009**, 21 (S1), 144-157.

[6] Hong, Y-C.; et al. Asian Dust Storm and Pulmonary Function of School Children in Seoul. *Science of the Total Environment*. **2010**, 408, 754-759.

[7] Hunt, A.; Abraham, J.L.; Toxicologic and Epidemiologic Clues from the Characterization of the 1952 London Smog Fine Particulate Matter in Archinal Autopsy Lung Tissues. *Environmental Health Perspectives*. **2003**, 111 (9), 1209-1214.

[8] Cilwa, K.E.; McCormack, M.C.; Lew, M.M.; Robitaille, C.I.; Corwin, L.; Malone, M.A.; Coe, J.V. Scatter-Free, Infrared Absorption Spectra of Individual, 3-5 μm, Airborne Dust Particles using Plasmonic Metal Microarrays: A Library of 63 Spectra. *Journal of Physical Chemistry*. Submitted.

[9] Oberdörster, G.; et al. Translocation of Inhaled Ultrafine Particles to the Brain. *Inhalation Toxicology*. **2004**, 16, 437-445.

[10] Hao, J.; Li, G.; Pang, B. Evidence for Cigarette Smoke-Induced Oxidative Stree in the Rat Pancreas. **2009**, 21 (12), 1007-1012.

[11] Williams, C.D.; Potts, R.J.; Steichen, T.J.; Doolittle, D.J.; Ayres, P.H. Upper Airways Sensory Irritation Responses of Mice Exposed to Mainstream Smoke from Four Cigarette Types. *Inhalation Toxicology*. **2010**, 22 (1), 49-55.

[12] Kane, D.B.; Asgharian, B.; Price, O.T.; Rostami, A.; Oldham, M.J. Effect of Smoking Parameters on the Particle Size Distribution and Predicted Airway Deposition of Mainstream Cigarette Smoke. *Inhalation Toxicology*. **2010**, 22 (3), 199-209.

[13] Roy, A.A.; Baxla, S.P.; Gupta, T.; Bandyopadhyaya, R.; Tripathi, S.N. Particles Emitted from Indoor Combustion Sources: Size Distribution Measurement and Chemical Analysis. *Inhalation Toxicology*. **2009**, 21 (10), 837-848.

[14] Morandi, M.T.; Ward, T.J.; et al. Wood Smoke Rick Assessment: Defining the Questions. *Inhalation Toxicology*. **2010**, 22 (2) 94-98.